A study of the flow boiling heat transfer in a minichannel for a heated wall with surface texture produced by vibration-assisted laser machining

Magdalena Piasecka[1], Kinga Strąk[2], Beata Maciejewska[3] and Bogusław Grabas[4]
[1,2,4] Faculty of Mechatronics and Mechanical Engineering,
[3] Faculty of Management and Computer Modelling,
Kielce University of Technology, Al. 1000-lecia P.P. 7, PL-25-314 Kielce, Poland

E-mail: [1]tmpmj@tu.kielce.pl

Abstract. The paper presents results concerning flow boiling heat transfer in a vertical minichannel with a depth of 1.7 mm and a width of 16 mm. The element responsible for heating FC-72, which flowed laminarly in the minichannel, was a plate with an enhanced surface. Two types of surface textures were considered. Both were produced by vibration-assisted laser machining. Infrared thermography was used to record changes in the temperature on the outer smooth side of the plate. Two-phase flow patterns were observed through a glass pane. The main aim of the study was to analyze how the two types of surface textures affect the heat transfer coefficient. A two-dimensional heat transfer approach was proposed to determine the local values of the heat transfer coefficient. The inverse problem for the heated wall was solved using a semi-analytical method based on the Trefftz functions. The results are presented as relationships between the heat transfer coefficient and the distance along the minichannel length and as boiling curves. The experimental data obtained for the two types of enhanced heated surfaces was compared with the results recorded for the smooth heated surface. The highest local values of the heat transfer coefficient were reported in the saturated boiling region for the plate with the type 1 texture produced by vibration-assisted laser machining.

1. Introduction

Heat transfer in small channels has been dealt with significant attention over the last few years, especially for application to for cooling compact devices. Due to the technological growth, methods allowing the intensification of the heat transfer are sought. Application of enhanced surfaces for cooling compact devices could allow additional intensification of heat transfer. The heat exchangers with small dimension channels enable meeting opposite requirements i.e. obtaining a potential large heat flux although the temperature difference between a heated surface and saturated liquid is small, in heat exchange systems of a small dimensions.

Many researchers have been carried out study on flow boiling heat transfer and pressure drop in micro- and minichannels [1-13] over the last twenty years. There are a lot of papers focused on pool boiling heat transfer on modified heated surfaces [14-17]. In their earlier works [17-20] the authors studied flow boiling heat transfer in minichannels where the working fluid was heated by an enhanced surface produced by laser surface texturing or electromachining (spark erosion). The literature also includes works concerned with porous structures [21,22], micro-structures in flow boiling [23] and

pool boiling [24]. References [25,26] focus on the use of porous surfaces to enhance flow boiling heat transfer in minichannels.

Among others, an increase in heat transfer enhancement resulting from producing micro- or mini-recesses on the heated surface corresponds to the increase in the number of nucleation sites. The presence of the recesses also contributes to an increase in the surface-to-volume ratio [14,17,19,20]. In order to increase the heat transfer enhancement, various technological processes which modify heated surfaces by means of passive or active methods. The extensive research on passive methods shows that modifying the characteristics and structure of the surface results in higher energy-efficiency and material savings. The properties and structure of a heated surface can be modified using chemical, thermal, mechanical or combined mechanical and thermal processes. The thermal processes include laser surface texturing, electromachining (spark erosion), sintering, electric arc spraying or plasma spraying. Thermal processes, such as: laser surface texturing were used in for processing the surfaces [27-30]. In [31] a vibration-assisted laser surface texturing of metals as a passive method for heat transfer enhancement was described. An evaluation of the use of laser-vibration melting to increase the surface roughness of metal objects was discussed in [32]. This paper presents the results of flow boiling heat transfer in a minichannel with an enhanced plate surface obtained by the vibration-assisted laser surface texturing. The main aim is to analyze the effects of the enhanced plate surface texture produced by vibration-assisted laser machining on the heat transfer coefficient in two boiling regions: the subcooled boiling region and the saturated boiling region.

2. Experimental stand and methodology, calculation of the heat transfer coefficient

2.1. Experimental stand

The study was carried out for a flow boiling process by using the experimental setup shown in figure 1a. It consists of several systems: the main loop with working fluid (Fluorinert FC-72), the data and image acquisition system with and the lighting system, the supply and control system.

The essential part of the main loop is a tested module with a minichannel (1). The main loop is also composed of: a gear pump (2), a compensating tank (3), a tube-type heat exchanger (4), a filter (5), a Coriolis mass flowmeter (6) and a deaerator (7). The data and image acquisition system designed to collect measurement data is made up of: an infrared camera E60 FLIR (15), a Canon EOS 550D digital SLR camera (16) and two data acquisition stations (DaqLab 2005 and MCC SC-1608G). The lighting system is high power LEDs (17) to light two phase flow. The accuracy of the IR camera was ± 1 °C or ± 1% in the temperature range: 0 – 120 °C and ± 2 °C or ± 2 % outside the range 0 – 120 °C. The supply and control system consists of an inverter welder, a shunt, an ammeter and a voltmeter.

In the tested module there is a vertical minichannel (8) with a single-sided enhanced heated plate surface (10). The minichannel has the dimensions: 1.7 mm (depth), 16 mm (width) and 180 mm (length). The heated element for FC-72 flowing in a minichannel is a Haynes-230 alloy plate (9), thickness of about 0.45 mm. In the experimental series, the plates in contact with the fluid in the channel had surfaces enhanced by vibration-assisted laser texturing. Two plates differing in texture were analyzed. In an additional series, a smooth plate was also used. Temperature of the heated plate on the outer side (the smooth surface not contacting fluid in the minichannel) was measured by infrared thermography, in the central, axially symmetric part of the channel. The plate was coated with black paint of emissivity about 0.83 [33,34]. The two-phase flow structures were observed through the glass pane (11) at the enhanced side of the plate being in contact with the fluid. At the inlet and outlet of the minichannel, pressure converters and K-type thermocouples were installed (12).

The two types of surface texture generated by vibration-assisted laser texturing are shown in figure 1b and c. They were produced at different parameters: one at a higher laser head speed of 5 m/min and a higher power of 1500 W (type 1 texture - figure 1b), and the other at a lower laser head speed of 2.5 m/min and a lower power of 1 250 W (type 2 texture - figure 1c). One texture is clearer with cavities deeper and more widely spaced, whereas the other texture is less clear with more shallow cavities and overlapping tracks.

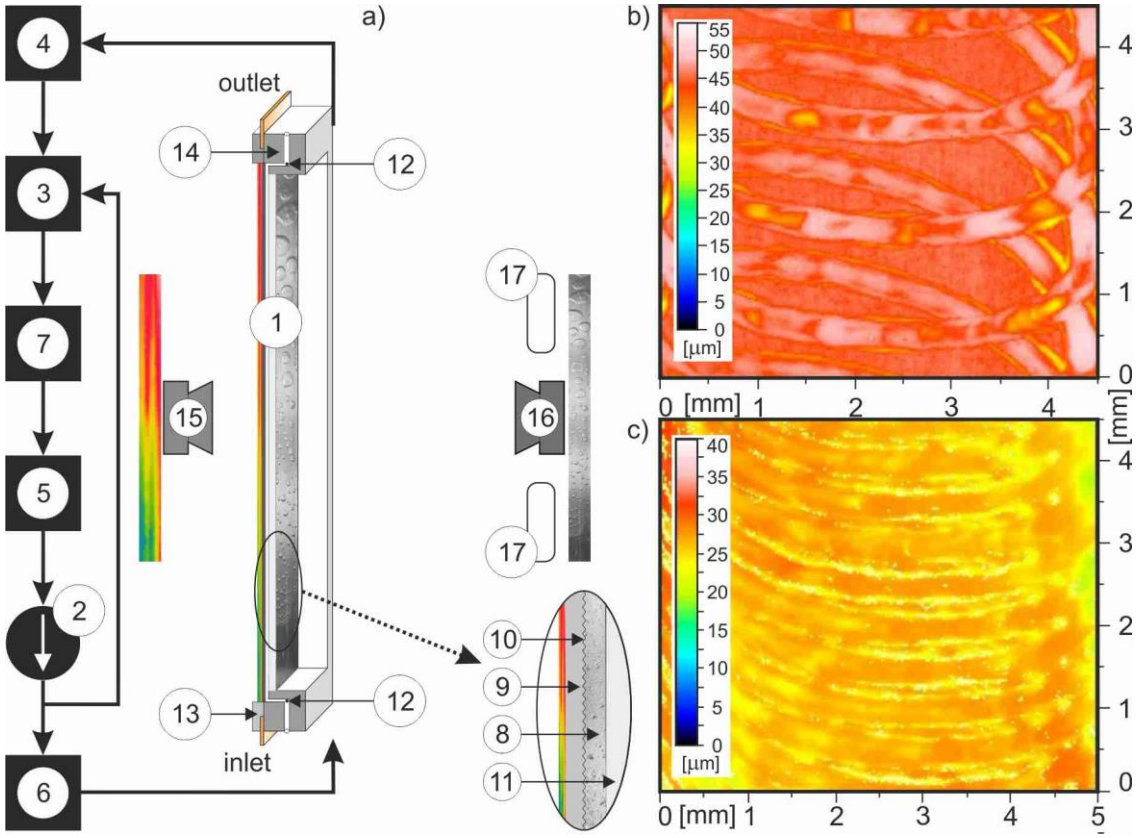

Figure 1. (a) Schematic diagram of the experimental setup, 1-test module with a minichannel; 2-gear pump; 3-compensating tank; 4-heat exchanger, 5-filter, 6-mass flowmeter, 7-deaerator, 8-minichannel, 9-heated plate, 10-enhanced surface of the plate, 11-glass pane, 12-thermocouple and pressure converter, 13-front cover, 14-channel body, 15-infrared camera; 16-digital SLR camera, 17-high power LEDs (400 W); **(b,c)** images of the foil surface produced by vibration-assisted laser texturing: **b)** type 1 texture, **c)** type 2 texture.

2.2. Experimental methodology

Three experimental series were performed to study the laminar flow of FC-72 in a minichannel for three heated plates differing in surface texture. Two surfaces enhanced by vibration-assisted laser texturing and a smooth surface was tested at similar thermal and flow parameters.

After the desired values of the pressure and flow rate were fixed, the electric power supplied to the heated plate was increased gradually to achieve an increase in the heat flux transferred to the fluid in the minichannel. It caused a change in the heat transfer between the plate surface and the working fluid from single phase convection to nucleate boiling. The process began with the onset of nucleate boiling and subcooled boiling. In the subcooled boiling region, the liquid was superheated at the interface with the plate and subcooled at the flow core. The saturated nucleate boiling occurred when the liquid reached its saturation temperature at the flow core.

2.3. Calculation of the heat transfer coefficient

The local heat transfer coefficients were calculated from: the equation (1) - for the subcooled boiling region or the equation (2) - for the saturated boiling region, as follows:

$$\alpha(x) = -\lambda \frac{\partial T(x,\delta)}{\partial y} \left(T(x,\delta) - T_f(x)\right)^{-1} \tag{1}$$

$$\alpha(x) = -\lambda \frac{\partial T(x,\delta)}{\partial y} \left(T(x,\delta) - T_{sat}(x)\right)^{-1} \tag{2}$$

where λ − coefficient of thermal conductivity of the heated plate, δ − plate thickness, $T(x,y)$ − plate temperature, x − coordinate relating to the fluid flow direction, y − coordinate relating to the thickness of the heated plate, $T_f(x)$ – fluid temperature determined on the basis of the linear distribution of fluid temperature along the minichannel length, $T_{sat}(x)$ – saturation temperature determined on the basis of the linear distribution of pressure along the minichannel length.

The average uncertainties of the relative heat transfer coefficient for the minichannel were 36.5 % [34]. The plate temperature T was determined by solving the inverse problem [35] of the heat transfer, described by Poisson's equation:

$$\frac{\partial^2 T}{\partial x^2} + \frac{\partial^2 T}{\partial y^2} = -\frac{I \cdot \Delta U}{A \cdot \delta \cdot \lambda} = -\frac{q_v}{\lambda} \quad \text{for } (x,y) \in \Omega \tag{3}$$

where $\Omega = \{(x,y) \in R^2 : 0 < x < L, \quad 0 < y < \delta\}$, L − length of the minichannel, q_v − volumetric heat flux, I − current, ΔU − voltage drop, A − surface area of the heated plate. The boundary conditions were shown in figure 2, where: P − number of measurements obtained using infrared thermography on the outer surface of heated plate, T_p − plate temperature measured by infrared thermography at the boundary $y=0$, $q_{w,loss}$ - heat loss to the surroundings, estimated as in [34] and λ , δ defined as for equations (1) and (2).

In domain Ω, the temperature T was approximated by means of the linear combination of Trefftz functions:

$$T(x,y) = u(x,y) + \sum_{i=1}^{N} a_i v_i(x,y) \tag{4}$$

where: $u(x,y)$ - particular solution of equation (3), $v_i(x,y)$ - the Trefftz functions [36-39].

The unknown coefficients α_i were calculated by minimizing the appropriate functional.

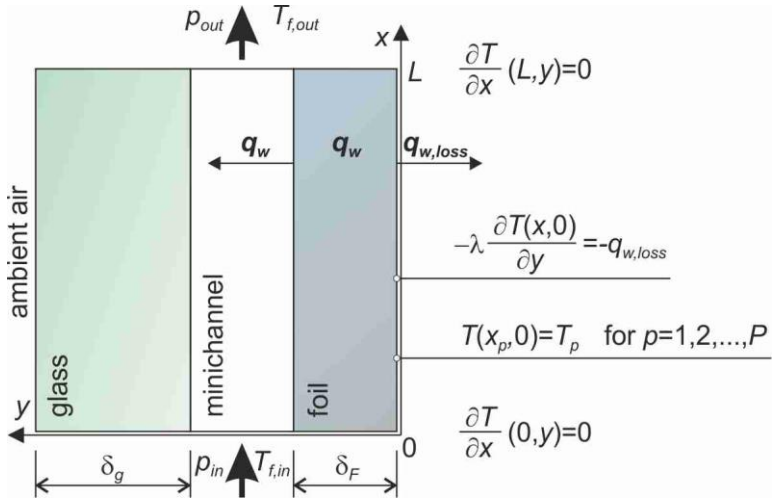

Figure 2. Boundary conditions for a two-dimensional approximation.

3. Results

The results are represented graphically as a relationship between the heat transfer coefficient and the distance from the minichannel inlet in figure 3 to compare the heat transfer on the enhanced plates with that on the smooth plate. Separate plots were generated for the subcooled boiling region (figure 3a) and the saturated boiling region (figure 3b), both refer to three different heat flux values (q_w). The values of the local heat transfer coefficient calculated for the enhanced plates and the smooth

plate were marked as green points (type 1 texture), blue points (type 2 texture) and red points (the smooth plate), respectively.

In the subcooled boiling region, the heat transfer coefficient was relatively low. The local values of the heat transfer coefficient increased slightly with the distance from the minichannel inlet. At the highest heat flux supplied to the plate, the local values of the heat transfer coefficient were the lowest for the surface enhanced by type 2 texture and the highest for the type 1 texture (figure 3a). In the analyzed boiling region, the data obtained for the enhanced plates did not differ significantly from that reported for the smooth surface. In the saturated boiling region (figure 3b), the heat transfer coefficient was very high for all the heated plates, with values up to a hundred times greater than those obtained for the subcooled boiling region. In this boiling region, there no data was recorded for type 2 texture because of the large fluctuations in the temperature of the heated surface in relation to the saturation temperature. The results reveal that locally there was no saturated boiling region. This is the reason why the data shown refers only to the plate with enhanced surface (type 1 texture) and the smooth plate. The lowest values of the coefficient were observed at the channel inlet and outlet. It was evident that heat transfer reported for the enhanced surface - type 1 texture - was more intensive than for the smooth surface in this boiling region. The presence of little cavities distributed over the whole surface of the heated element, is likely to have contributed to the formation of numerous nucleation sites. Reference [40] reports that when a bubble departs from an enhanced surface, the interface between the liquid and the vapour occurs in the subsurface capillaries, where it is unaffected by the cold temperature of the liquid above. As the subsurface capillaries are interconnected, the vapour produced within the subsurface structure at one site tends to activate other sites. The analysis of the data indicates that the use of the type 1 texture with a sparser spacing of artificial pores was very beneficial. The very close spacing between the artificial cavities constituting the type 2 texture was responsible for the large fluctuations in the temperature of the heated surface and the instability of boiling heat transfer in the saturated boiling region causing a considerable drop in heat transfer.

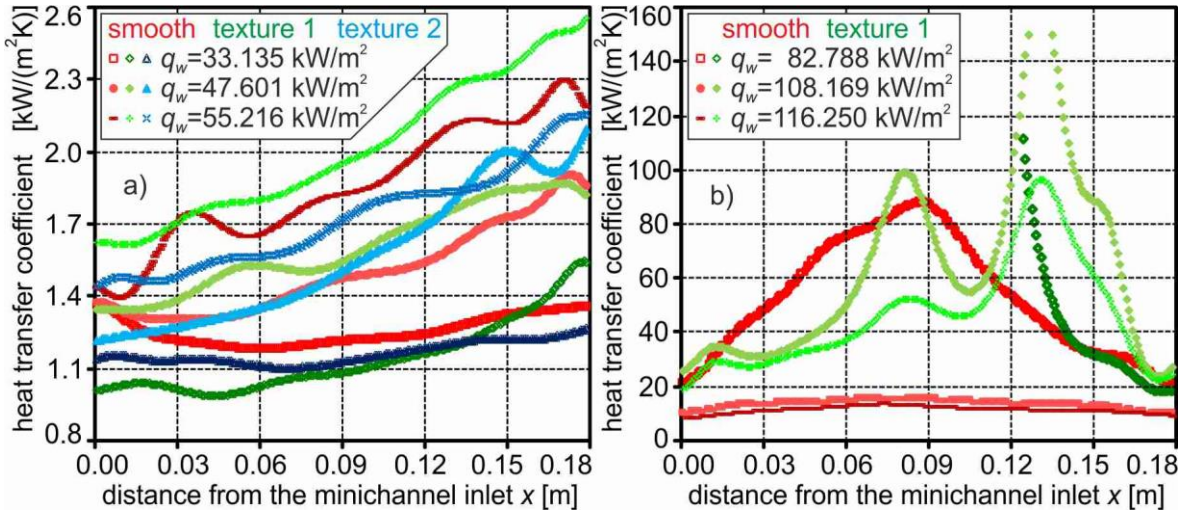

Figure 3. Heat transfer coefficient vs. the minichannel length, data for: **(a)** the subcooled boiling region, **(b)** the saturated boiling region; experimental parameters average mass flux of 273 kg/(m^{2}s), average inlet pressure of 125 kPa, average inlet liquid subcooling of 44 K.

The boiling curves in figure 4 were plotted from the data collected during tests, which involved increasing the heat flux supplied to the heated plates. They showed the relationship between the heat flux q_w and the difference in temperature T_p-T_f (figures 4a and c) or T_p-T_{sat} (figures 4b and d). All the boiling curves in figure 4 were generated for two selected distances from the minichannel inlet: 0.06 m and 0.15 m. The curves were drawn for the two enhanced surfaces and the smooth one. The results obtained for the three surfaces were plotted as green points, blue points and red points to represent the

plate with the type 1 texture, the plate with the type 2 texture, and the smooth plate, respectively. The boiling curves showing the relationship between the heat flux and the difference in temperature T_p-T_f are similar in shape, although the curve for the type 1 texture shifts by 5 K towards the higher values of the difference in temperature T_p-T_f in the region of the higher heat flux (figure 4c). These boiling curves show that there was a drop in temperature during the 'nucleation hysteresis' [18,41] at the onset of nucleate boiling (ONB). However, the boiling curves illustrating the heat flux versus the difference T_p-T_{sat} are not alike; the curve for the type 2 texture is particularly different; it differs from the other curves significantly and this results from the large fluctuations in temperature of the heated plate.

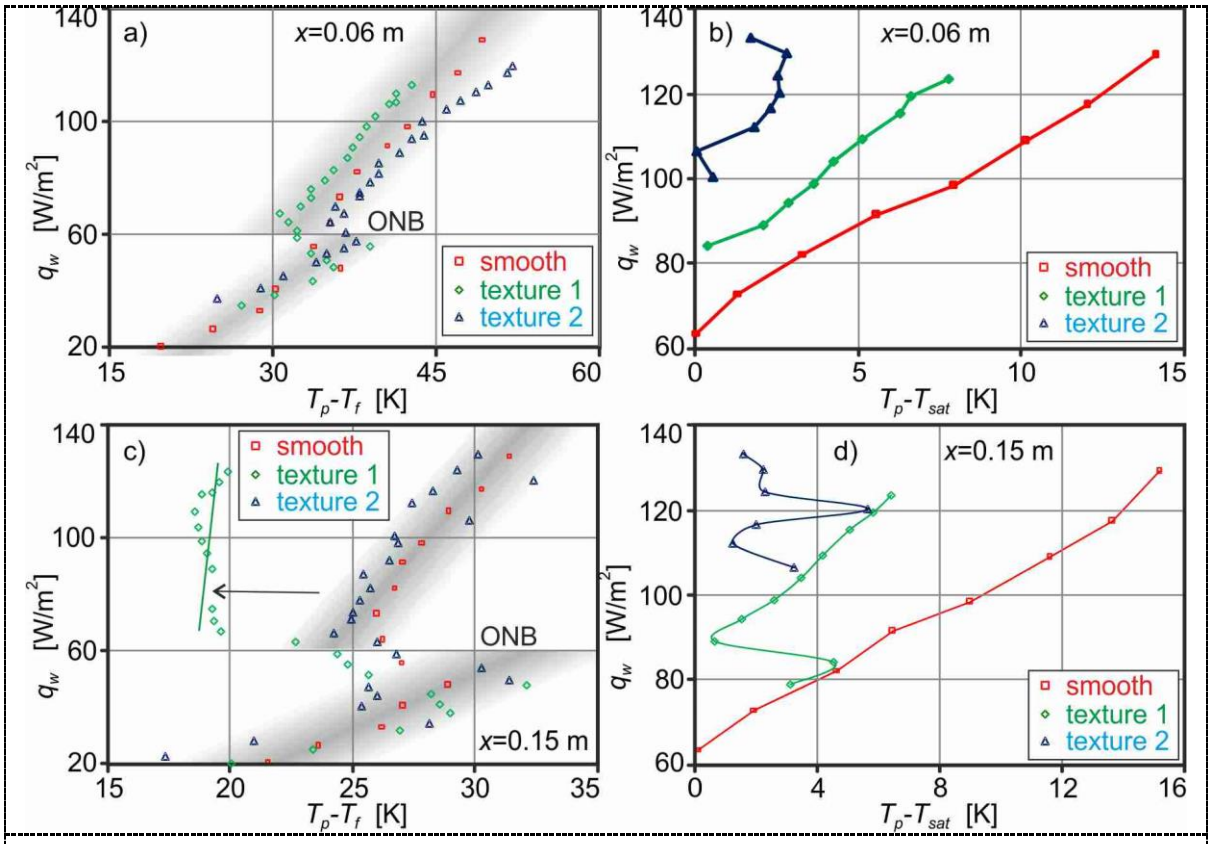

Figure 4. Boiling curves generated for two distances from the minichannel inlet: (**a)** 0.06 m, **(b)** 0.15 m; experimental parameters as for figure 3.

4. Conclusion

The paper presents results concerning flow boiling heat transfer in a vertical minichannel with a depth of 1.7 mm and a width of 16 mm. The element responsible for heating FC-72, which flowed laminarly in the minichannel, was a plate with an enhanced surface. Two types of surface textures were considered. Both were produced by vibration-assisted laser machining. Infrared thermography was used to record changes in the temperature on the outer smooth side of the plate. Two-phase flow patterns were observed through a glass pane. The main aim of the study was to analyze how the two types of surface textures affect the heat transfer coefficient. A two-dimensional heat transfer approach was proposed to determine the local values of the heat transfer coefficient. The inverse problem for the heated wall was solved using a semi-analytical method based on the Trefftz functions. The experimental data obtained for the two types of enhanced heated surfaces with surface texture produced by vibration-assisted laser machining was compared with that recorded for the smooth surface. The results were presented as relationships between the heat transfer coefficient and the distance along the minichannel length and as boiling curves. In the subcooled boiling region, the heat

transfer coefficient was relatively low. The values increased slightly with the distance from the minichannel inlet. In the saturated boiling region, the heat transfer coefficient was very high (with values up to a hundred times higher than those reported for the subcooled boiling region). The highest local values of the heat transfer coefficient were reported in the saturated boiling region for the plate with type 1 texture produced by vibration-assisted laser machining.

Acknowledgments
The research reported herein was supported by a grant from the National Science Centre (No. DEC-2013/09/B/ST8/02825).

References

[1] Cavallini A, Del Col D, Matkovic M and Rossetto L 2009 Frictional pressure drop during vapour-liquid flow in minichannels: Modelling and experimental evaluation *Int. J. Heat Fluid Flow* **30** 131–9
[2] Kandlikar S G 2002 Fundamental issues related to flow boiling in minichannels and microchannels *Exp. Therm. Fluid Sci.* **26** 389–407
[3] Mikielewicz D, Wajs J, Gliński M and Zrooga A B R S 2013 Experimental investigation of dryout of SES 36, R134a, R123 and ethanol in vertical small diameter tubes *Exp. Therm. Fluid Sci.* **44** 556–64
[4] Hu X, Lin G, Cai Y and Wen D 2011 Experimental study of flow boiling of FC-72 in parallel minichannels under sub-atmospheric pressure *Appl. Therm. Eng.* **31** 3839–53
[5] Kaew-On J, Sakamatapan K and Wongwises S 2011 Flow boiling heat transfer of R134a in the multiport minichannel heat exchangers *Exp. Therm. Fluid Sci.* **35** 364–74
[6] Bohdal T and Dutkowski K 2011 Investigations of heat transfer during subcooled flow boiling of refrigerants in minichannels *Ann. Set Environ.* **13** 409–23
[7] Phan H T, Caney N, Marty P, Colasson S and Gavillet J 2011 Flow boiling of water in a minichannel: The effects of surface wettability on two-phase pressure drop *Appl. Therm. Eng.* **31** 1894–905
[8] Grzybowski H and Mosdorf R 2014 Dynamics of pressure oscillations in flow boiling and condensation in the minichannel *Int. J. Heat Mass Transf.* **73** 500–10
[9] Ali R, Palm B and Maqbool M H 2011 Flow boiling beat transfer characteristics of a minichannel up to dryout condition *J. Heat Transf.* **133** 081501
[10] Liu Z and Bi Q 2015 Onset and departure of flow boiling heat transfer characteristics of cyclohexane in a horizontal minichannel *Int. J. Heat Mass Transf.* **88** 398–405
[11] Owhaib W, Palm B and Martin-Callizo C 2006 Flow boiling visualization in a vertical circular minichannel at high vapor quality *Exp. Therm. Fluid Sci.* **30** 755–63
[12] Zhang C, Chen Y, Wu R and Shi M 2011 Flow boiling in constructal tree-shaped minichannel network *Int. J. Heat Mass Transf.* **54** 202–9
[13] Boye H, Staate Y and Schmidt J 2007 Experimental investigation and modelling of heat transfer during convective boiling in a minichannel *Int. J. Heat Mass Transf.* **50** 208–15
[14] Pastuszko R and Piasecka M 2012 Pool boiling on surfaces with mini-fins and micro-cavities *J. Phys. Conf. Ser.* **395** 012137
[15] Pastuszko R and Wójcik T M 2015 Experimental investigations and a simplified model for pool boiling on micro-fins with sintered perforated foil *Exp. Therm. Fluid Sci.* **63** 34–44
[16] Jun S, Sinha-Ray S and Yarin A L 2013 Pool boiling on nano-textured surfaces *Int. J. Heat Mass Transf.* **62** 99–111
[17] Piasecka M 2014 Heat transfer research on enhanced heating surfaces in flow boiling in a minichannel and pool boiling *Ann. Nucl. Energy* **73** 282–93
[18] Hozejowska S and Piasecka M 2014 Equalizing calculus in Trefftz method for solving two-dimensional temperature field of FC-72 flowing along the minichannel *Heat Mass Transf.* **50** 1053–63

[19] Piasecka M 2014 Correlations for flow boiling heat transfer in minichannels with various orientations *Int. J. Heat Mass Transf.* **81** 114–21
[20] Piasecka M 2015 Impact of selected parameters on refrigerant flow boiling heat transfer and pressure drop in minichannels *Int. J. Refrig.* **56** 198–212
[21] El-Genk M S and Ali A F 2010 Enhanced nucleate boiling on copper micro-porous surfaces *Int. J. Multiph. Flow* **36** 780–92
[22] Pranoto I and Leong K C 2014 An experimental study of flow boiling heat transfer from porous foam structures in a channel *Appl. Therm. Eng.* **70** 100–14
[23] Ahn H S, Kang S H, Lee C, Kim J and Kim M H 2012 The effect of liquid spreading due to micro-structures of flow boiling critical heat flux *Int. J. Multiph. Flow* **43** 1–12
[24] Seo H, Chu J H, Kwon S Y and Bang I C 2015 Pool boiling CHF of reduced graphene oxide, graphene, and SiC-coated surfaces under highly wettable FC-72 *Int. J. Heat Mass Transf.* **82** 490–502
[25] Depczyński W 2014 Investigating porosity of sintering porous copper structure with 3D micro-focus X-ray computed tomography (μCT) *J. Achiev. Mater. Manuf. Eng.* **66** 67–72
[26] Depczyński W 2014 Sintering of copper layers with a controlled porous structure *METAL 2014 23rd Int. Conf. Metallurgy and Materials* ed C R Tanger LTD, Keltickova 62, Slezska, Ostrava 1219–24
[27] Radek N, Konstanty J and Scendo M 2015 The electro-spark deposited WC-Cu coatings modified by laser treatment *Arch. Metall. Mater.* **60** 2579-84
[28] Piasecka M 2014 Laser texturing, spark erosion and sanding of the surfaces and their practical applications in heat exchange devices *Adv. Mater. Res.* **874** 95–100
[29] Ameli M, Agnew B, Leung P S, Ng B, Sutcliffe C J, Singh J and McGlen R 2013 A novel method for manufacturing sintered aluminium heat pipes (SAHP) *Appl. Therm. Eng.* **52** 498–504
[30] Sommers A D and Yerkes K L 2013 Using micro-structural surface features to enhance the convective flow boiling heat transfer of R-134a on aluminum *Int. J. Heat Mass Transf.* **64** 1053–63
[31] Grabas B 2015 Vibration-assisted laser surface texturing of metals as a passive method for heat transfer enhancement *Exp. Therm. Fluid Sci.* **68** 499–508
[32] Grabas B 2015 An evaluation of the use of laser-vibration melting to increase the surface roughness of metal objects *Arch. Metall. Mater.* **60**
[33] Orzechowski T 2003 Heat transfer on ribs with microstructured surface *Monographs, studies, hearings, 39* (Kielce University of Technology)
[34] Piasecka M, Strąk K and Maciejewska B 2017 Calculations of flow boiling heat transfer in a minichannel based on Liquid Crystal and Infrared Thermography data *Heat Transf. Eng.* **38**
[35] Özisiḳ M N and Orlande H R B 2000 *Inverse heat transfer: fundamentals and applications* (New York.: Fundamentals and Applications, Taylor & Francis)
[36] Herrera I 2000 *Trefftz method: A general theory, numerical methods for partial differential equations* **16** 561–80
[37] Ciałkowski M J and Frąckowiak A 2002 Solution of the stationary 2D inverse heat conduction problem by Trefftz method *J. Therm. Sci.* **11** 148–62
[38] Grysa K and Maciejewska B 2013 Trefftz functions for the non-stationary problems *J. Theor. Appl. Mech.* **51** 251–64
[39] Grysa K, Maciąg A and Pawińska A 2012 Solving nonlinear direct and inverse problems of stationary heat transfer by using Trefftz functions *Int. J. Heat Mass Transf.* **55** 7336–40
[40] Webb R L and Kim N-H 2005 *Principles of enhanced heat transfer* ed Webb Ralph L (New York: Taylor & Francis)
[41] Piasecka M and Maciejewska B 2015 Heat transfer coefficient during flow boiling in a minichannel at variable spatial orientation *Exp. Therm. Fluid Sci.* **68** 459–67